JOURNAL OF MATERIALS SCIENCE 37 (2002) 2017–2022

Devitrification and microstructural coarsening of a fluoride-containing barium aluminosilicate glass

J. A. GRIGGS*,§,¶, K. J. ANUSAVICE*, J. J. MECHOLSKY, JR.‡
*Departments of *Dental Biomaterials and ‡Materials Science and Engineering, University of Florida, Gainesville, FL 32610, USA*
E-mail: JGriggs@tambcd.edu

Barium aluminosilicate (BAS) glass-ceramics have the potential to be used in the production of cast prostheses for biomedical applications because of their radiopacity and increased strength compared with traditional feldspathic porcelains. It is essential to understand the crystallization kinetics of these materials in order to fabricate products with increased fracture resistance rapidly. It was hypothesized that the addition of fluoride (F) to the composition of BAS glass would reduce the necessary processing time and temperatures by obviating the need for a separate crystal nucleation treatment. BASF glass was subjected to both linear non-isothermal and one-stage isothermal crystallization treatments, and the resulting glass-ceramics were characterized using x-ray diffraction, differential thermal analysis, and stereology. BASF glass had a low energy barrier to crystallization (397 kJ/mol) and transformed to $76 \pm 2\%$ crystallinity within 30 min at 975°C. A fine-grained microstructure was produced by bulk crystallization without the need for a separate crystal nucleation stage. After the initial crystal precipitation, the mean crystal size and mean free path between crystals increased over time at elevated temperature by a diffusion rate-limited coarsening mechanism.

1. Introduction

Glasses in the composition range 19–51 wt% BaO, 8–37 wt% Al_2O_3, and 31–66 wt% SiO_2 have the potential to be used in the production of biomedical prostheses as they can be cast into desired shapes and crystallized by thermal treatments to produce glass-ceramic composites [1, 2]. Barium aluminosilicate (BAS) glass-ceramics also have the potential for useful mechanical properties [1]. The hexacelsian crystalline phase, $BaO \cdot Al_2O_3 \cdot 2SiO_2$, that initially precipitates from these glasses has a structure similar to that of mica, which is responsible for the increased machinability of a glass-ceramic product for computer-aided design/manufacturing (CAD/CAM) applications (Dicor MGC) [3–5]. An understanding of the crystal nucleation and growth kinetics of these materials is essential in order to select rapid processing treatments that may result in products with increased fracture resistance.

Hexacelsian crystals have a higher average coefficient of thermal expansion (6.1 ppm/°C) compared with the monoclinic form of celsian (2.1 ppm/°C) [6]. Upon repeated thermal cycling, the volumetric change of hexacelsian glass-ceramics leads to the formation of microcracks that may be detrimental to mechanical properties. However, the formation of monoclinic celsian is slow and requires high processing temperatures. As a result, previous research on BAS glass-ceramics has been primarily focused on catalyzing the formation of monoclinic celsian glass-ceramics, which are more resistant to the thermal cycling conditions encountered in aerospace applications. In dental and orthopedic restorative applications, however, thermal cycling of this magnitude only occurs during processing. Thus, hexacelsian glass-ceramics with lower processing temperatures may serve as alternatives to monoclinic celsian glass-ceramics.

Previous researchers have reported that stoichiometric BAS glasses begin to precipitate the hexacelsian crystal phase and the monoclinic celsian phase upon heating to 900–980°C and 1040–1100°C, respectively [7–10]. In the case of hexacelsian precipitation, the crystals usually nucleate on the specimen surface because the energy barrier to surface crystallization is lower than that associated with bulk crystallization [1, 7, 11]. Mechanical activation of oxide precursors results in an increased proportion of the hexacelsian phase because of increased surface area of the reactant

§*Present Address*: Department of Biomaterials Science, Baylor College of Dentistry—a member of the Texas A&M University System Health Science Center, 3302 Gaston Avenue, Dallas, TX 75246, USA.
¶Author to whom all correspondence should be addressed.

powders [12]. Bulk crystal nucleation and a finer microstructure have been achieved by adding a crystal nucleation stage at 850°C prior to the crystal growth treatment [1]. The conversion of hexacelsian to monoclinic celsian crystals at lower temperatures has been accomplished by seeding with monoclinic celsian crystals [2, 6, 13] and by partial substitution of SrO for BaO in the glass [6, 8, 9]. The substitution of Ga_2O_3 or GeO_2 for Al_2O_3 also aids in the formation of monoclinic celsian but results in reduced strength of the final product [13]. Increasing the Al_2O_3 content of the parent glass increases strength, while addition of Li_2O decreases strength [2]. In the case of increased Al_2O_3 content, mullite, hexacelsian, and monoclinic celsian phases have been detected in the microstructure. In addition to amorphous reactants, mixtures of crystalline metal oxides [6, 13], barium-exchanged zeolites [14, 15], and sol-gels [2, 9, 10] have also been successfully used for the production of BAS ceramics.

The production of a glass-ceramic material typically involves a multistage crystallization treatment in which a time-consuming crystal nucleation stage is necessary to achieve a high crystal density in the final product. Previous studies [5, 16] have reported that fluoride-containing glasses undergo discrete phase separation upon casting, resulting in saturation of the matrix glass with heterogeneous nucleation sites. The purpose of the present study was to characterize the crystallization kinetics of a fluoride-containing barium aluminosilicate (BASF) glass. It was hypothesized that autonucleation of BASF glass would reduce processing time by obviating the need for a separate crystal nucleation stage.

2. Experimental procedure

2.1. Glass preparation

Glass frit with a composition of 31.9 wt% SiO_2, 20.1 wt% Al_2O_3, 22.0 wt% BaO, 8.43 wt% MgO, 2.97 wt% CaO, 8.23 wt% MgF_2, and 6.42 wt% P_2O_5 was produced by the Specialty Glass Company (Oldsmar, FL, USA). At least 5.23 wt% MgF_2 was required for low melt viscosity and rapid crystallization. An extra 3 wt% MgF_2 was added to compensate for the anticipated volatilization during melting. The frit was placed in a covered zirconia-reinforced platinum crucible (Johnson Matthey, Seabrook, NH, USA) and melted in an electric furnace (Model DT-31-RS-OS, Deltech, Inc., Denver, CO, USA) at 1500°C for 1 h. The glass was cast into custom graphite molds (5.1 × 12.7 × 2.1 cm). The glass ingots were annealed in an electric furnace (Model F6020, Thermolyne Corporation, Dubuque, IA, USA) at 600°C for 1 h and then furnace cooled to room temperature.

The glass ingots were sectioned into rectangular bars (24 mm in length and 6 mm wide) using a low-speed diamond saw (Model 650, South Bay Technology Inc., San Clemente, CA, USA). The glass bars were ground against a 75 μm metal-bonded diamond abrasive disk (3M Abrasive Systems Division, St. Paul, MN, USA) to achieve a thickness of 3.5 mm. Two glass bars were ground in a mortar and pestle to produce powders. The glass powders were sieved to isolate particles less than 710 μm in diameter for composition analyses. The composition analyses were performed by Coors Ceramics Analytical Laboratory (Golden, CO, USA) by acid dissolution of glass powders followed by inductively coupled plasma spectroscopy and pyrohydrolysis (Table I).

TABLE I Composition of BASF glass prior to melting and after casting

Component	Composition (wt%)		
	As-received frit	Melt I	Melt II
SiO_2	31.9	32.1	31.9
Al_2O_3	20.1	20.4	20.1
BaO	22.0	21.9	22.0
MgO	8.43	9.07	9.73
MgF_2	8.23	7.00	6.86
P_2O_5	6.42	6.37	6.43
CaO	Remainder	Remainder	Remainder
Total	100	100	100

2.2. X-ray diffraction

Twelve glass bar specimens were heated from 25 to 1050°C at 5°C/min in an electric furnace (Model F6020, Thermolyne Corporation, Dubuque, IA, USA). Beginning at 675°C, two specimens were removed from the furnace and bench cooled at 15-min (75°C) intervals. Annealed glass specimens were used as a control. Using a mortar and pestle, each specimen was ground and the powder was sieved to include only particles less than 30 μm diameter, which were then mixed with amyl acetate. The resulting slurries were mounted on glass microscope slides and analyzed in an x-ray diffractometer (APD3720, Philips Electronic Instruments Inc., Mahwah, NJ, USA) with a Cu K_α radiation source. Scans were conducted at an intensity of 1000 counts/min over a 2θ range of 10° to 120° at 5°/min.

2.3. Differential thermal analysis

Glass powder was also sieved to isolate 710–850 μm particles. This particle size range was chosen to minimize surface crystallization while maintaining adequate contact area for heat conduction between particles. Powder specimens weighing 15 mg each were placed in platinum pans under 100 mL/min of flowing dry air in a differential thermal analyzer (TG/DTA 320, Haake-Seiko Inc., Paramus, NJ, USA). Each specimen was heated from 25 to 1000°C at a rate (β) of 5, 10, 20, 30, 40, or 50°C/min. The difference in heat absorption between the specimen and a sapphire reference material was measured. The peak difference in heat absorption was determined as the temperature corresponding to maximum rate of crystal growth, T_P. A corrected Ozawa-Chen method was used to estimate the energy barrier to crystallization [17]. This method involves linear regression of $\ln(T_P/\beta)$ versus $1/T_P$, where the slope of the regression line represents the energy barrier to crystallization, E_C, divided by the universal gas constant, R.

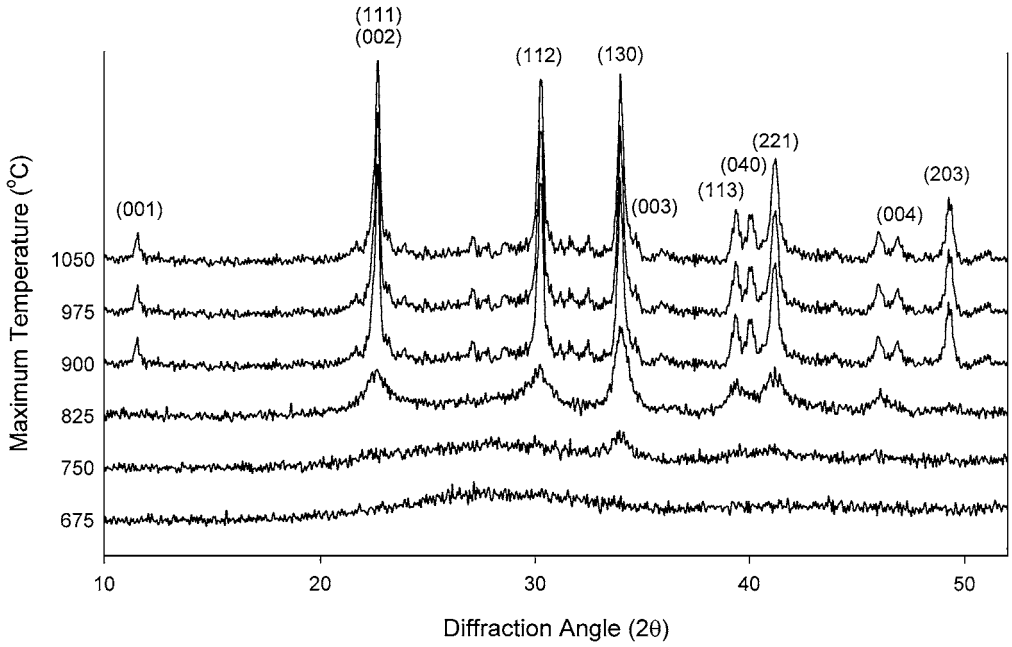

Figure 1 X-ray diffraction spectra of BASF glass-ceramic specimens crystallized by linear non-isothermal treatment and quenched from 675, 750, 825, 900, 975, and 1050°C.

2.4. Microstructural analysis

Twenty glass bar specimens were divided into one control group and four treatment groups of four specimens each. The specimens in treatment groups were crystallized by one-stage isothermal treatments at 975°C for 0.5, 4, 32, or 256 h to form glass-ceramics. Isothermal treatments were performed in an electric tube furnace (Model 54577, Lindberg Corporation, Watertown, WI, USA). After crystallization, glass-ceramic specimens were annealed at 600°C for 1 h and furnace cooled to room temperature. The control group of glass specimens received no crystallization treatment, but they were subjected to the same annealing treatment as the glass-ceramic specimens.

Each specimen was sectioned at 90° and 45° angles to the long axis. The sections were polished to a 0.05 μm finish using an alumina abrasive slurry and acid etched using 1% aqueous hydrofluoric acid for 10 s to reveal their microstructures. Two stereological fields measuring 5×5 μm were scanned from each section using an atomic force microscope (Nanoscope III Scanning Probe Microscope, Digital Instruments, Inc., Santa Barbara, CA, USA) in the tapping mode for a total of 16 fields for each of the five groups.

The mean crystalline volume fraction and mean free path between crystals were calculated for each treatment group according to standard stereological techniques [18]. The mean crystal diameter, thickness, and aspect ratio were calculated using formulas for stereology of circular plate-shaped crystals [19] and applying a correction factor for the average diameter of a hexagonal plate as follows:

$$\bar{d}_{\text{hex}} = \frac{2}{\pi} \int_0^{\frac{\pi}{2}} 2r_{\text{hex}} d\theta \approx 0.909 d_{\text{circ}}$$

where r_{hex} is the radius of a hexagonal plate, $\bar{d}_{\text{hex}}$ is the apparent diameter of the hexagonal plate averaged over all possible angles of cross section, and d_{circ} is the equivalent diameter of a circular plate with the same average cross section.

3. Results

3.1. X-ray diffraction

Powder diffraction spectra of non-isothermally treated specimens quenched from 675, 750, 825, 900, 975, and 1050°C are shown in Fig. 1. No diffraction peaks were present in specimens quenched from 675°C. Diffraction peaks corresponding to the hexacelsian crystal phase were detected in all other treatment groups and increased in intensity with increasing treatment temperature. No other crystalline phases were present in detectable quantities.

3.2. Differential thermal analysis

As shown in Fig. 2, glass powders exhibited symmetric exothermic crystallization peaks. The peak

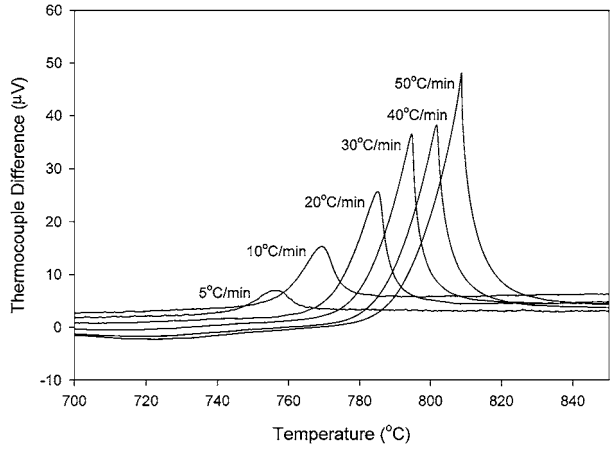

Figure 2 Exothermic response of BASF glass powder to differential thermal analysis at heating rates of 5, 10, 20, 30, 40, and 50°C/min.

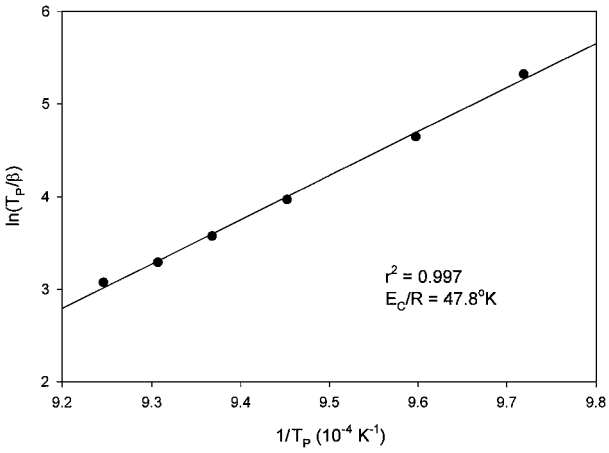

Figure 3 Logarithmic regression of heating rate, β, versus exothermic peak temperature, T_P, to determine the energy barrier to crystallization, E_C, for BASF glass.

crystallization temperature shifted to higher temperatures with increasing rate of heating. The peak crystallization temperatures (T_P) were 756, 769, 785, 795, 802, and 809°C for heating rates (β) of 5, 10, 20, 30, 40, and 50°C/min, respectively. Fig. 3 shows the linear regression graph of $\ln(T_P/\beta)$ versus $1/T_P$. The thermal analysis data closely followed the corrected Ozawa-Chen solution to the Johnson-Mehl-Avrami model ($r^2 = 0.997$). BASF glass had a low energy barrier to crystallization (397 kJ/mol).

3.3. Microstructural analysis

The crystals present in all glass-ceramic specimens exhibited hexagonal plate morphology. As this shape appears similar to a lath-like morphology in cross section, high-magnification examination of fracture surfaces was required to confirm the plate geometry (Fig. 4). No crystals were present in the untreated glass specimens. BASF glass rapidly transformed to $76 \pm 2\%$ crystallinity within 30 min of treatment at 975°C, and the crystalline volume fraction remained constant thereafter.

Atomic force micrographs in Fig. 5a–d show representative microstructures of specimens treated for (a) 0.5, (b) 4, (c) 32, and (d) 256 h. The hexacelsian crystals in each specimen group had a bimodal size distribution, and the mean crystal size increased with increasing crystallization time at 975°C (Fig. 6). The mean crystal diameters were 0.25 ± 0.04, 0.52 ± 0.05, 0.96 ± 0.17, and 1.76 ± 0.25 μm for the 0.5, 4, 32, and 256 h treatment groups, respectively. These data closely follow a cubic power law model ($r^2 = 0.992$), *i.e.*, an eight-fold increase in processing time was necessary to double the mean crystal size. The mean crystal aspect ratio was 3.8 ± 0.4 and was independent of treatment duration ($p = 0.41$). The mean free path between crystals was 0.073 ± 0.004, 1.0 ± 0.1, 1.9 ± 0.3, and 2.4 ± 0.5 μm for treatment durations of 0.5, 4, 32, and 256 h, respectively.

4. Discussion

Uno *et al.* [20] reported the formation of a barium fluoromica ($BaMg_6Si_6Al_2O_{20}F_4$) crystal phase from the same composition of glass as used in the present study. However, only the hexacelsian phase ($BaO \cdot Al_2O_3 \cdot 2SiO_2$) was detected in the present study. The crystal morphologies of the two phases are similar, but the x-ray diffraction spectra are quite different. Uno *et al.* employed isothermal crystallization treatments in the same temperature range as those used in the present study. The composition of fluorine-containing glasses changes slightly during melting as SiF_6 is volatilized at high temperatures, but it is unlikely that the crystal phase discrepancy was caused by

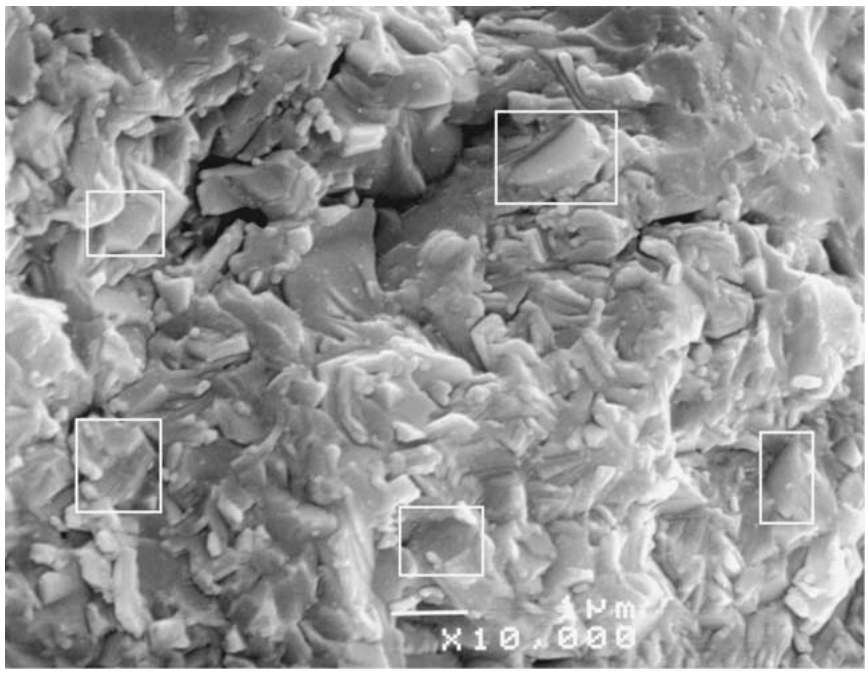

Figure 4 Scanning electron micrograph of a fractured surface of a BASF glass-ceramic after isothermal crystallization treatment at 975°C for 32 h. Some of the exposed crystals are marked with white boxes.

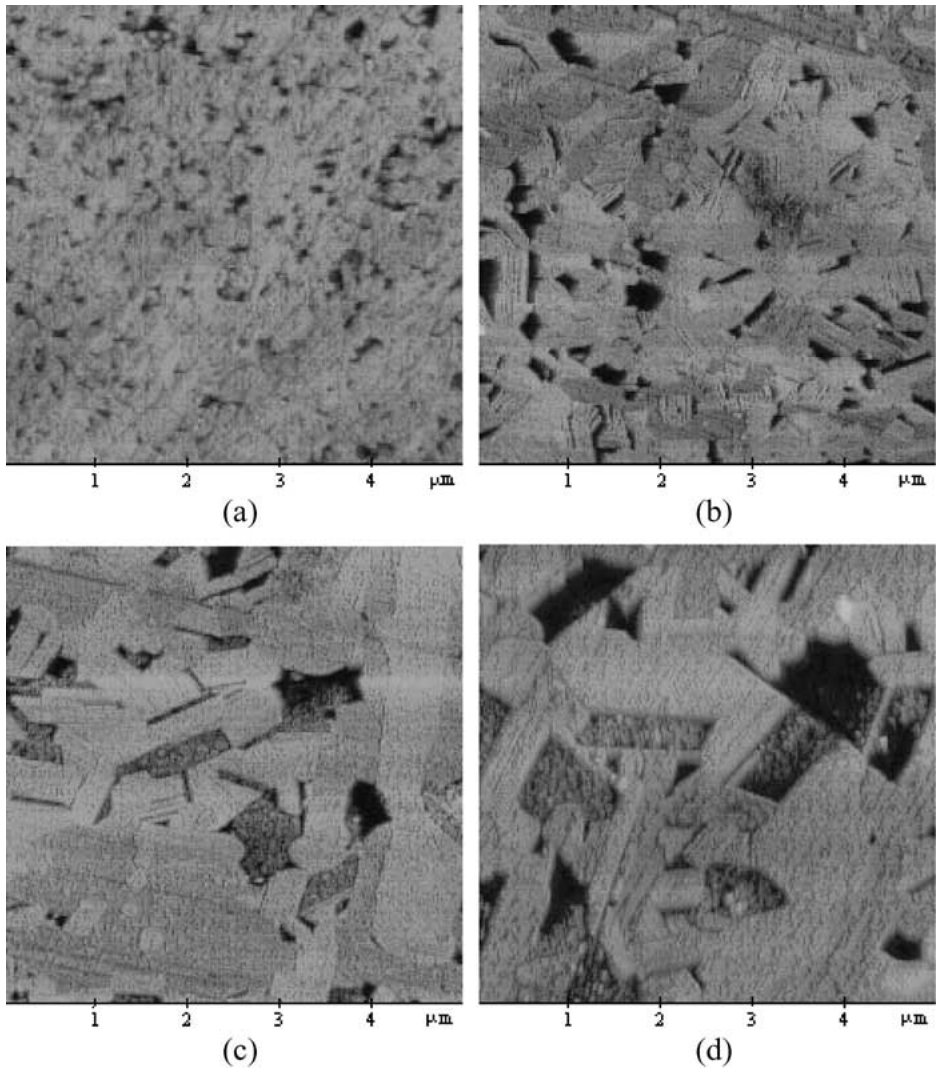

Figure 5 Atomic force micrographs of polished and acid-etched sections of BASF glass-ceramics after isothermal crystallization treatments at 975°C for (a) 0.5 h, (b) 4 h, (c) 32 h, and (d) 256 h.

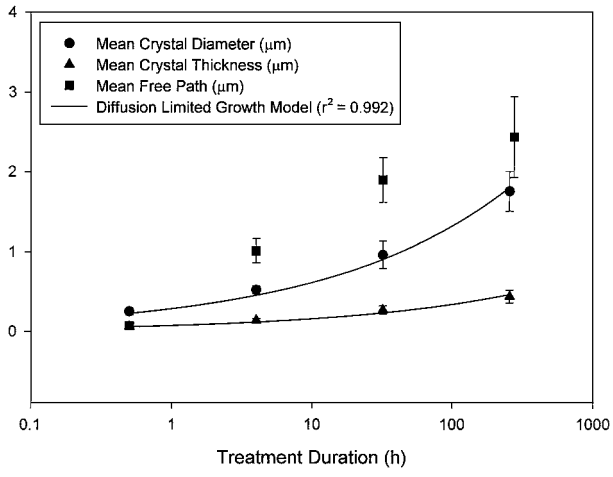

Figure 6 Mean free path, mean crystal diameter, and mean crystal thickness of BASF glass-ceramics after isothermal crystallization treatments at 975°C for 0.5, 4, 32, and 256 h. The diffusion limited growth model was determined by fitting mean crystal diameter and thickness values to a cubic power law.

such a minor composition difference (Table I). Other researchers have reported the formation of monoclinic celsian crystals from stoichiometric BAS glass [7] and strontium-substituted BAS glasses [9] at the maximum temperature investigated in the present study (1050°C). However, the transformation to monoclinic celsian is slow, and the BASF specimens were quenched immediately upon reaching the maximum temperature, allowing little time for this transformation to occur.

The energy barrier to crystallization for BASF glass (397 kJ/mol) was lower than that found previously for stoichiometric BAS glass (543 kJ/mol) [7]. This was probably caused by discrete phase separation upon casting and the resultant saturation of the glass with heterogeneous nucleation sites as reported for other fluorine-containing glasses [5, 16]. Based on this evidence, no separate crystal nucleation stage was used for the isothermal treatments in the present study. Stoichiometric BAS glass is reported to crystallize from the specimen surface without a nucleation stage [7]. Such a lack of bulk crystallization results in coarse-grained microstructures and possibly inferior mechanical properties. However, fine-grained bulk crystallization of BASF glass was achieved in spite of eliminating this step. The low energy barrier is also evident from rapid crystallization at low processing temperatures. The peak crystallization rate of powder specimens was at 756°C for a heating rate of 5°C/min, and 76%

crystallization occurred within 30 min at 975°C for monolithic specimens. This is in contrast to stoichiometric and strontium substituted BAS glasses, which have peak crystallization temperatures of 1017°C and 1002°C for powder specimens and 1120°C and 1075°C, respectively, for monolithic specimens measured at a heating rate of 5°C/min [8].

After the initial precipitation of fine-grained hexacelsian crystals, the mean crystal size of BASF glass-ceramics increased over time at elevated temperatures. Previous studies have reported the same phenomenon in calcium fluoride glass-ceramics [16] and fluoromica glass-ceramics [21]. In these cases, the initial microstructures were modified by a dissolution and reprecipitation coarsening mechanism. It was suggested that addition of fluorine to the glass composition increases ionic mobility and makes this coarsening mechanism possible. For a diffusion limited growth rate, the mean crystal size should follow a cubic power law with respect to treatment duration [22]. The crystal size data for BASF glass-ceramics closely follow such a relationship ($r^2 = 0.992$).

The proportion of glass phase in the BASF glass-ceramics remained constant as the mean crystal size increased, causing an increase in mean free path between crystals (Fig. 6). The observed changes in microstructure have important implications for the mechanical properties of the final glass-ceramic. Larger reinforcing crystals may better deflect cracks as they propagate through the material, resulting in increased fracture resistance [23]. However, an excessively large crystal size may lead to thermally induced spontaneous microcracking throughout the material, resulting in decreased fracture resistance [24]. Future research should focus on the effects of microstructure, *i.e.*, grain size and shape, on the fracture toughness and strength of BASF glass-ceramics.

5. Conclusion

Fluorine-containing barium aluminosilicate (BASF) glass crystallized rapidly at low processing temperatures relative to stoichiometric BAS glass. It was possible to eliminate a separate crystal nucleation stage and still achieve fine-grained bulk crystallization using a one-stage isothermal treatment. BASF glass-ceramic microstructures coarsened following the initial precipitation of crystals. This change in microstructure may have important effects on the mechanical properties of these materials.

Acknowledgment

This study was supported by NIH-NIDCR grants DE09307, DE06672, and DE07234.

References

1. C. H. I. DRUMMOND and N. P. BANSAL, *Ceram. Eng. Sci. Proc.* **11** (1990) 1072.
2. W. ZHOU, L. ZHANG and J. YANG, *J. Mater. Sci.* **32** (1997) 4833.
3. J. Y. THOMPSON, S. C. BAYNE and H. O. HEYMANN, *J. Prosthet. Dent.* **76** (1996) 619.
4. I. M. PETERSON, S. WUTTIPHAN, B. R. LAWN and K. CHYUNG, *Dent. Mater.* **14** (1998) 80.
5. C. K. CHYUNG, G. H. BEALL and D. G. GROSSMAN, in "Electron Microscopy and Structure of Materials," edited by G. Thomas (University of California Press, Berkeley, 1972) p. 1167.
6. I. G. TALMY, D. A. HAUGHT and E. J. WUCHINA, *International SAMPE Electronics Conference* **6** (1992) 687.
7. N. P. BANSAL and M. J. HYATT, *J. Mater. Res.* **4** (1989) 1257.
8. M. J. HYATT and N. P. BANSAL, *J. Mater. Sci.* **31** (1996) 172.
9. N. FRÉTY, A. TAYLOR and M. H. LEWIS, *J. Non-Cryst. Solids* **195** (1996) 28.
10. K. J. D. MACKENZIE and T. KEMMITT, *Therm. Acta* **325** (1999) 5.
11. N. P. BANSAL, M. J. HYATT and C. H. I. DRUMMOND, *Ceram. Eng. Sci. Proc.* **12** (1991) 1222.
12. S. BOSKOVIC, D. KOSANOVIC, D. BAHLOUL-HOURLIER, P. THOMAS and K. S., in Ninth World Round Table Conference on Sintering, Belgrade, Yugoslavia, 1999, edited by B. D. Stojanovic, V. V. Skorokhod and M. V. Nikolic (Kluwer Academic/Plenum Publishers, Belgrade, Yugoslavia, 1999) p. 167.
13. J. A. ZAYKOSKI and I. G. TALMY, *Ceram. Eng. Sci. Proc.* **15** (1994) 779.
14. S. BOSKOVIC, D. KOSANOVIC, V. DONDUR and R. DIMITRIJEVIC, *Ceram. Int.* **26** (2000) 33.
15. G. DELLAGLI, C. FERONE, M. C. MASCOLO and M. PANSINI, *Solid State Ionics* **127** (2000) 309.
16. Q. A. JUMA'A and J. M. PARKER, in "Nucleation and Crystallization in Glasses," edited by J. H. Simmons, D. R. Uhlmann and G. H. Beall (The American Ceramic Society, Washington, D.C., 1981) p. 218.
17. H. YINNON and D. R. UHLMANN, *J. Non-Cryst. Solids* **54** (1983) 253.
18. J. E. HILLIARD, in "Quantitative Microscopy," edited by F. N. Rhines and R. T. Dehoff (McGraw-Hill, India, 1968) p. 45.
19. R. L. FULLMAN, *AIME Trans.* **197** (1953) 447.
20. T. UNO, T. KASUGA and S. NAKAYAMA, *J. Cer. Soc. Jap.* **100** (1992) 315.
21. D. G. GROSSMAN, *J. Amer. Ceram. Soc.* **55** (1972) 446.
22. G. W. GREENWOOD, *Acta Metall.* **4** (1956) 243.
23. K. T. FABER and A. G. EVANS, *ibid.* **31** (1983) 565.
24. A. G. EVANS and K. T. FABER, *J. Amer. Ceram. Soc.* **67** (1984) 255.

Received 17 April
and accepted 21 December 2001